Nonlinearity of strong interaction and doorway states for one-nucleon transfer reactions

B.L. Birbrair[a] and V.I. Ryazanov

Petersburg Nuclear Physics institute Gatchina, 188300 St. Petersburg, Russia

Abstract. The experimental data on the doorway states for one-nucleon transfer reactions permit to reveal the many-particle nucleon-nucleon forces resulting from the nonlinearity of strong interaction. The three-particle and four-particle forces are found to be of the same magnitude as the two-particle ones in contrast to the finding from the few-nucleon systems. The origin of this difference is explained.

1 Introduction: nonlinearity of strong interaction and many-particle nucleon-nucleon forces

There is no doubts at present that the physics of strong interaction is essentially nonlinear. The immediate consequence of this nonlinearity is the existence of many-particle nucleon-nucleon forces. Indeed, the Lagrangian density of nonlinear theory contains higher-power terms of meson fields in addition to the quadratic ones. There are φ^3 and φ^4 terms in renormalizable theories and those of arbitrary powers in the effective ones. The φ^3 term describes the emission of meson by meson as shown in fig. 1a. This gives rise to the three-particle nucleon-nucleon force when each meson line enters the nucleon one, fig. 1b. In the second perturbation order the process of fig. 1c appears leading to the four-particle force, the φ^4 term, fig. 1d, gives rise to such a force at first perturbation order, and so on. In this sense the nonlinearity of strong interaction and the existence of many-particle nucleon-nucleon forces is the same.

As shown by practice of the calculations for few-nucleon systems the three-particle NN forces must be included in addition to the two-particle ones to get the good agreement with experiment. But the $3N$ forces are found to be rather modest compared to the $2N$ ones: the overall effect is within 10% only [1]. According to the conventional opinion little room remains for the $4N$ forces. To justify this viewpoint the following estimate is used which

 ᵃ e-mail: `birbrair@thd.pnpi.spb.ru`
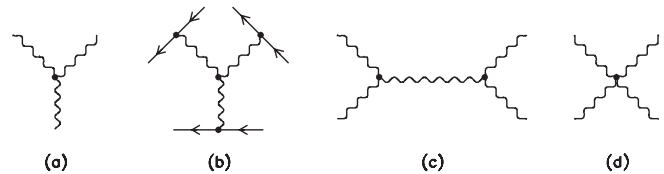
Fig. 1. The φ^3 term (a), the resulting $3N$ forces (b), the second-order process in φ^3 (c), and the φ^4 term (d), both giving rise to the $4N$ forces.

is based on the effective field theory arguments [2]:

$$f_2 \simeq 30\,\text{MeV}, \qquad f_3 \simeq \frac{f_2^2}{m} \simeq 1\,\text{MeV},$$

$$f_4 \simeq \frac{f_2^3}{m^2} \simeq 30\,\text{keV}, \tag{1}$$

where f_2, f_3 and f_4 are the $2N, 3N$ and $4N$ forces at the average distance between nucleons, m is the nucleon mass. So

$$f_2 : f_3 : f_4 \ = \ 1 : 10^{-3/2} : 10^{-3}. \tag{2}$$

It is worth mentioning, however, that the processes of figs. 1c and 1d give rise to the $4N$ forces when each meson line enters its own nucleon one as shown in fig. 2a. But the interaction is not instantaneous and therefore two meson lines may enter the same nucleon one, fig. 2b. This gives rise to the contribution of the $4N$ interaction mechanism to the $3N$ force. Clearly the higher forces may contribute to the $3N$ interaction by this mechanism. The two following points must be stressed:

1. What the few-nucleon people assume to be the $3N$ forces is in fact the combination of the genuine ones arising

Fig. 2. The $4N$ force (a) and the contribution of the $4N$ interaction mechanism to the $3N$ force (b). The circles denote the unification of fig. 1c and fig. 1d processes.

Fig. 3. Contributions of $2N$ (a), $3N$ (b) and $4N$ (c) forces to the nuclear static field. The ellipsis denotes the possible contributions from higher forces.

from the nonlinearity, fig. 1b, and the contributions of higher many-particle forces (the example is provided by fig. 2b).

2. These two sources of the $3N$ forces cannot be separated with the aid of the data on few-nucleon systems because some ansatz for both the wave functions and the forces must be used in this case.

Such separation becomes possible by studying the doorway states for one-particle transfer reactions in complex nuclei. As demonstrated in ref. [3] these states are eigenstates of the nucleon in nuclear static field the only contribution to which being provided by the Hartree diagrams with the free-space nucleon-nucleon forces as shown in fig. 3. The demonstration is repeated in sect. 2.1.

It is of primary importance that the $2N$ contribution, fig. 3a,

$$U_2(x) = \int f_2(|\mathbf{r} - \mathbf{r}'|)\rho(r')\mathrm{d}^3\mathbf{r}' \qquad (3)$$

is independent of any nuclear model because the $2N$ forces f_2 are deduced from the properties of the deuteron and the NN elastic-scattering data, whereas the nucleon density distributions are determined from the electron-nucleus [4] and 1 GeV proton-nucleus [5] elastic-scattering data. Owing to this independence the contribution of many-particle NN forces to the nuclear static field can be unambiguously revealed by comparing the results of calculations including the $2N$ forces only (*i.e.* only $U_2(x)$) with the observed doorway state energies. The latter ones are observed as average energies of the peaks in the quasielastic knockout $(p,2p)$, (p,pn), $(e,e'p)$ reaction cross-sections as functions of the missing energy. The data are obtained by the PNPI group [6] for the $(p,2p)$ and (p,pn) reactions in the doubly closed-shell nuclei ^{16}O, ^{40}Ca, ^{90}Zr, and ^{208}Pb. These nuclei are spherical, hence the quantum-mechanical problem is the motion of a particle in the central field. This problem is solved with any desired accuracy and without any simplifying approximations. So the doorway states under consideration are unique nuclear objects, both model-independent and obeying exactly soluble problem. For this reason a lot of reliable information about both the many-particle NN forces and the nuclear structure may be obtained by studying this object. These results are summarized in subsect. 2.2. The number of nucleons which are out of the nuclear Fermi-surface because of the correlations is estimated in subsect. 2.3 by using the fact that the doorway state wave functions describe the single-particle states of nucleons rather than those of quasiparticles, thus
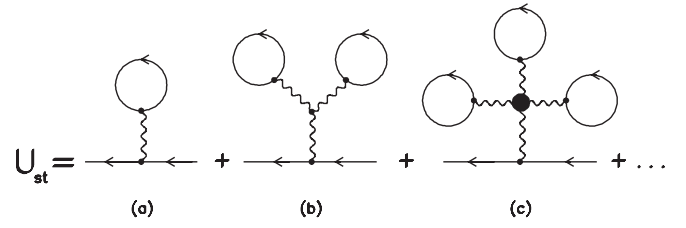
being correlation-free objects. Section 3 is for concluding remarks.

2 Doorway states for one-nucleon transfer reactions

2.1 Theory

Evolution of the state arising from the one-nucleon transfer to the nuclear ground state $|A_0\rangle$ at the initial time moment $t = 0$ is described by the single-particle propagator [7]

$$\begin{aligned} S(x,x';\tau) &= -i\langle A_0|T\psi(x,\tau)\psi^\dagger(x',0)|A_0\rangle = \\ &= i\theta(-\tau)\sum_j^{(A-1)} \Psi_j(x)\Psi_j^\dagger(x')e^{-iE_j\tau} \\ &\quad -i\theta(\tau)\sum_k^{(A+1)} \Psi_k(x)\Psi_k^\dagger(x')e^{-iE_k\tau}. \end{aligned} \qquad (4)$$

At $\tau < 0$ it describes the evolution of the hole state,

$$\Psi_j(x) = \langle (A-1)_j|\psi(x)|A_0\rangle, \quad E_j = \mathcal{E}_0(A) - \mathcal{E}_j(A-1), \qquad (5)$$

when the nucleon is removed from the ground state A_0, whereas at $\tau > 0$ the evolution of the particle state is described,

$$\Psi_k(x) = \langle A_0|\psi(x)|(A+1)_k\rangle, \quad E_k = \mathcal{E}_k(A+1) - \mathcal{E}_0(A), \qquad (6)$$

when the nucleon is added to the ground state A_0. The quantities $\mathcal{E}_j(A-1)$, $\mathcal{E}_k(A+1)$ and $\mathcal{E}_0(A)$ are total binding energies of the states $|(A-1)_j\rangle$ of the $(A-1)$ nucleus, the states $|(A+1)_k\rangle$ of the $(A+1)$ nucleus and the ground state $|A_0\rangle$ of the A one.

The Fourier transform of the propagator

$$G(x,x';\varepsilon) = \int S(x,x';\tau)e^{i\varepsilon d\tau} =$$

$$\sum_j^{(A-1)} \frac{\Psi_j(x)Psi_j^\dagger(x')}{\varepsilon - E_j - i\delta} + \sum_k^{(A+1)} \frac{\Psi_k(x)\Psi_k^\dagger(x')}{\varepsilon - E_k + i\delta}, \quad \delta \to +0 \ (7)$$

obeys the Dyson equation

$$\begin{aligned} \varepsilon G(x,x';\varepsilon) &= \delta(x-x') + \hat{k}_x G(x,x';\varepsilon) \\ &\quad + \int M(x,x_1;\varepsilon)G(x_1,x';\varepsilon)\mathrm{d}x_1, \qquad (8) \end{aligned}$$
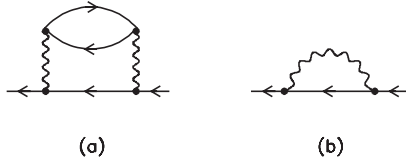
Fig. 4. Lowest-order energy-dependent diagrams of the mass operator: the correlation one (a) and the Fock one (b).

where $\hat{k}_x$ is the kinetic energy and the mass operator $M(x, x'; \varepsilon)$ includes all Feynman diagrams which are irreducible in the one-particle channel.

We are interested in the very beginning of the evolution, *i.e.* the $\tau \to 0$ limit. According to the time-energy Heisenberg relation this is equivalent to the limit $\varepsilon \to \infty$. In this limit

$$G(x, x'; \varepsilon) = \frac{I_0(x, x')}{\varepsilon} + \frac{I_1(x, x')}{\varepsilon^2} + \frac{I_2(x, x')}{\varepsilon^3}, \quad (9)$$

where (see the definition (4) of the propagator)

$$I_0(x, x') = \sum_j^{(A-1)} \Psi_j(x)\Psi_j^\dagger(x') + \sum_k^{(A+1)} \Psi_k(x)\Psi_k^\dagger(x') =$$
$$i\left[S(x, x'; +0) - S(x, x'; -0) \right]; \quad (10)$$

$$I_1(x, x') = \sum_j^{(A-1)} E_j \Psi_j(x)\Psi_j^\dagger(x') + \sum_k^{(A+1)} E_k \Psi_k(x)\Psi_k^\dagger(x') =$$
$$-\left[\dot{S}(x, x'; +0) - \dot{S}(x, x'; -0) \right]; \quad (11)$$

$$I_2(x, x') = \sum_j^{(A-1)} E_j^2 \Psi_j(x)\Psi_j^\dagger(x') + \sum_k^{(A+1)} E_k^2 \Psi_k(x)\Psi_k^\dagger(x') =$$
$$-i\left[\ddot{S}(x, x'; +0) - \ddot{S}(x, x'; -0) \right], \quad (12)$$

the quantities I_0, I_1 and I_2 thus describing the very beginning of the evolution $\left(\dot{S} = \frac{\partial S}{\partial \tau}, \ddot{S} = \frac{\partial^2 S}{\partial \tau^2} \right)$.

Now consider the mass operator $M(x, x'; \varepsilon)$. It includes the energy-independent Hartree diagrams $U_{\rm st}(x)\delta(x - x')$ which are shown in fig. 3, the higher-order diagrams describing the nuclear correlation effects (the lowest-order diagram of such kind is shown in fig. 4a) and the Fock ones, fig. 4b. The correlation diagrams include the propagators of intermediate states thus behaving as ε^{-1} in the $\varepsilon \to \infty$ limit (see ref. [8] for a more stringent demonstration). The same is valid for the Fock diagrams, fig. 4b. Indeed, the interaction between baryons proceeds via the exchange by some particles (they are quark-antiquark pairs and/or gluons in the QCD) and therefore both the momentum and the energy are transferred through the interaction. As a result the Fock diagrams also include the intermediate-state propagators thus being of order of ε^{-1} in the $\varepsilon \to \infty$ limit. (In ref. [3] this is demonstrated for the meson-nucleon in-

termediate state.) So the mass operator in this limit is

$$M(x, x'; \varepsilon) = U_{\rm st}(x)\delta(x - x') + \frac{\Pi(x, x')}{\varepsilon} + \cdots \quad (13)$$
$$\varepsilon \to \infty$$

Introducing the static Hamiltonian

$$h_{\rm st} = \hat{k}_x + U_{\rm st}(x), \quad (14)$$

let us write down the high-energy limit Dyson equation in the form

$$\varepsilon G(x, x'; \varepsilon) = \delta(x - x') + h_{\rm st} G(x, x'; \varepsilon)$$
$$+ \int \left(\frac{\Pi(x, x_1)}{\varepsilon} + \cdots \right) G(x_1, x'; \varepsilon) {\rm d}x_1. \quad (15)$$

Putting the asymptotics (9) into (15) and equating coefficients at the same powers of ε^{-1}, we get

$$\sum_j^{(A-1)} \Psi_j(x)\Psi_j^\dagger(x') + \sum_k^{(A+1)} \Psi_k(x)\Psi_k^\dagger(x') =$$
$$\delta(x - x'), \quad (16)$$

$$\sum_j^{(A-1)} E_j \Psi_j(x)\Psi_j^\dagger(x') + \sum_k^{(A+1)} E_k \Psi_k(x)\Psi_k^\dagger(x') =$$
$$h_{\rm st}\delta(x - x'), \quad (17)$$

$$\sum_j^{(A-1)} E_j^2 \Psi_j(x)\Psi_j^\dagger(x') + \sum_k^{(A+1)} E_k^2 \Psi_k(x)\Psi_k^\dagger(x') =$$
$$h_{\rm st}^2\delta(x - x') + \Pi(x, x'). \quad (18)$$

Equations (11), (14) and (17) may be written as

$$-\left[\dot{S}(x, x'; +0) - \dot{S}(x, x'; -0) \right] =$$
$$h_{\rm st}\delta(x - x') = [k_x + U_{\rm st}(x)]\delta(x - x'). \quad (19)$$

As follows from the lhs of (19) the Hamiltonian $h_{\rm st}$ describes the very beginning of the one-nucleon transfer process, the eigenstates of $h_{\rm st}$ thus being the doorway states for one-nucleon transfer reactions. On the other hand, the rhs of (19) shows that the Hamiltonian $h_{\rm st}$ describes the motion of nucleon in nuclear static field $U_{\rm st}(x)$. Indeed, the latter is expressed through the free-space NN forces rather than the effective ones, thus being the nucleon field rather than the quasiparticle one. So we proved that the doorway states for one-nucleon transfer reactions are the eigenstates of nucleon in nuclear static field.

Let us introduce the doorway state wave functions

$$h_{\rm st}\varphi_\lambda(x) = \varepsilon_\lambda\varphi_\lambda(x) \quad (20)$$

and write down eqs. (16)–(18) in the doorway state representation. Multiplying them by $\varphi_\lambda^\dagger(x)\varphi_\lambda(x')$ and integrating over x and x', we get

$$\sum_j^{(A-1)} s_j^{(\lambda)} + \sum_k^{(A+1)} s_k^{(\lambda)} = 1, \quad (16a)$$

Fig. 5. Experimental doorway state energies and results of the calculations using the Bonn B (a) and OSBEP (b) potentials for the 2N forces. The label "pair" is for the results including the 2N forces only, whereas those including both the two-particle and many-particle forces are labelled by "full".

$$\sum_j^{(A-1)} E_j s_j^{(\lambda)} \; + \; \sum_k^{(A+1)} E_k s_k^{(\lambda)} \; = \; \varepsilon_\lambda \; , \qquad (17a)$$

$$\sum_j^{(A-1)} E_j^2 s_j^{(\lambda)} \; + \; \sum_k^{(A+1)} E_k^2 s_k^{(\lambda)} \; = \; \varepsilon_\lambda + \sigma_\lambda^2 \; , \qquad (18a)$$

where

$$s_{j,k}^{(\lambda)} \; = \; \left| \int \Psi_{j,k}^\dagger(x) \varphi_\lambda(x) \mathrm{d}x \right|^2 \qquad (21)$$

is the fraction of the doorway state λ in the actual nuclear state j or k, and σ_λ is its spreading width

$$\sigma_\lambda^2 \; = \; \int \varphi_\lambda^\dagger(x) \Pi(x, x') \varphi_\lambda(x') \mathrm{d}x \, \mathrm{d}x' \; . \qquad (22)$$

Let us discuss the above relations in more details.

1. As follows from eq. (16a) the doorway states of nucleus A are distributed over the physical states of both the $A-1$ and $A+1$ nuclei. This is a general property of single-particle states of arbitrary nature because it follows from the commutation relation

$$a_\alpha^\dagger a_\alpha + a_\alpha a_\alpha^\dagger \; = \; 1 \qquad (23)$$

for the fermion field operators (the subscript α labels the single-particle state of any nature). Indeed,

$$\langle A_0 | a_\alpha^\dagger a_\alpha | A_0 \rangle + \langle A_0 | a_\alpha a_\alpha^\dagger | A_0 \rangle =$$

$$\sum_j^{(A-1)} \langle A_0 | a_\alpha^\dagger | (A-1_j) \rangle \langle (A-1)_j | a_\alpha | A_0 \rangle \; +$$

$$+ \sum_k^{(A+1)} \langle A_0 | a_\alpha | (A+1)_k \rangle \langle (A+1)_k | a_\alpha^\dagger | A_0 \rangle \; =$$

$$\sum_j^{(A-1)} s_j^{(\alpha)} + \sum_k^{(A+1)} s_k^{(\alpha)} \; = \; 1 \; . \qquad (24)$$

This is the actual physical reason why the single-particle occupation numbers

$$n_\alpha \; = \; \langle A_0 | a_\alpha^\dagger a_\alpha | A_0 \rangle \; = \; \sum_j^{(A-1)} s_j^{(\alpha)} \qquad (25)$$

are less than unity in the general case. According to the arguments of ref. [9] $n_\alpha < 1$ because the high-momentum

components of nuclear single-particle spectral function

$$s_\alpha(\varepsilon) \;=\; \sum_{j}^{(A-1)} s_j^{(\alpha)} \, \delta(\varepsilon - E_j) \qquad (26)$$

are not available in experiment. As seen from (24) and (25) these arguments are wrong.

2. As seen from (22) the doorway state spreading widths depend upon the wave functions rather than the energies, thus being roughly the same for all doorway states (there is no arguments in favour of the momentum dependence of the $\Pi(x,x')$ operator). In such conditions it is reasonable to identify σ with the largest observed width value. The latter is the width of the peaks corresponding to the $1s_{1/2}$ hole states. According to ref. [6] measurements it is 20 MeV in all nuclei.

3. The absolute values of the s-factors which are necessary to determine the doorway state energies using the relation (17a) are measured with a rather poor accuracy because of both the experimental and theoretical uncertainties. For this reason the energies of weakly bound states with $|\varepsilon_\lambda| < \sigma$ are yet unknown (one should bear in mind that the low-lying states of $A\mp1$ nuclei are Landau-Migdal [8] quasiparticles rather than the nucleon single-particle states). The situation is more favourable for deep hole states $|\varepsilon_\lambda| > \sigma$, since they are mainly distributed over the physical states of the $A-1$ nucleus, and therefore the contribution from the second term of the lhs of eq. (17a) may be neglected. For these reasons the average energies of the peaks in the cross-sections of the quasielastic knockout reactions leading to the deep hole states can be identified with the doorway state energies within an accuracy of 2–3 MeV. In this case the relative s-factors, which are believed to be more reliable than the absolute ones, are sufficient.

2.2 Results

The calculations with the $2N$ forces only are performed using two different NN potentials: the Bonn B [10] and the OSBEP [11] ones. In both cases the static field is found to consist of the Lorentz scalar and the Lorentz vector with values of about -400 MeV and $+300$ MeV, respectively, *i.e.* just those provided by the Dirac phenomenology [12]. In this way nuclear relativity is found to be a really existing nuclear phenomenon rather than the suggestion of J.D. Walecka [13]. So the eigenstate equation (20) is the Dirac equation, the eigenfunctions $\varphi_\lambda(x)$ thus being Dirac bispinors (see ref. [3] for details).

The experimental doorway state energies are shown in fig. 5 together with the results of the calculations. As seen from the figure the calculated "pair" spectra are constricted compared to the observed ones: the lowest states are underbound, whereas the highest ones are overbound in most of the cases. This means that the potential well resulting from the $2N$ forces is too wide but insufficiently deep thus clearly indicating the presence of the contribution from many-particle NN forces. To get the deeper and
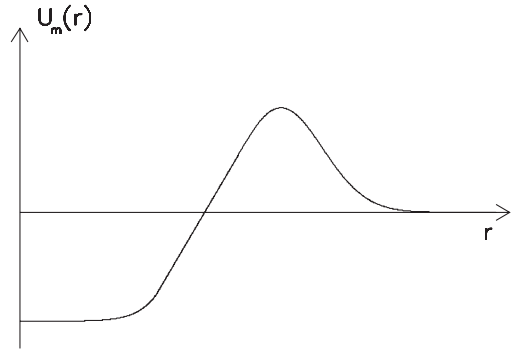
Fig. 6. Contribution U_m of many-particle forces to the nuclear static field (schematic plot).

narrower potential well, this contribution must be negative in the nuclear interior and positive in the nuclear surface region as schematically shown in fig. 6. Nothing is known about the many-particle NN forces resulting from the nonlinearity of strong interactions. Under such conditions it is reasonable to look for $U_m(r)$ as a power series expansion in the nuclear density distribution,

$$U_m(r) \;=\; a_3\rho^2(r) + a_4\rho^3(r) + \cdots \qquad (27)$$

the ρ^2 and ρ^3 terms arising from the $3N$ and $4N$ forces, etc. To elucidate the physical meaning of the coefficients, let us consider a general form of the $3N$ term:

$$U_3(r) \;=\; \int f_3(\mathbf{r}_1 - \mathbf{r}, \mathbf{r}_2 - \mathbf{r})\rho(\mathbf{r}_1)\rho(\mathbf{r}_2)\mathrm{d}^3\mathbf{r}_1\mathrm{d}^3\mathbf{r}_2 \;. \qquad (28)$$

In the homogeneous nuclear matter this gives

$$U_3 \;=\; \rho^2 \int f_3(\mathbf{r}_1 - \mathbf{r}, \mathbf{r}_2 - \mathbf{r}) \, \mathrm{d}^3\mathbf{r}_1\mathrm{d}^3\mathbf{r}_2 \;, \qquad (29)$$

so

$$a_3 \;=\; \int f_3(\boldsymbol{\xi},\boldsymbol{\eta}) \, \mathrm{d}^3\boldsymbol{\xi}\mathrm{d}^3\boldsymbol{\eta} \;. \qquad (30)$$

In the same way

$$a_4 \;=\; \int f_4(\boldsymbol{\xi},\boldsymbol{\eta},\boldsymbol{\zeta}) \, \mathrm{d}^3\boldsymbol{\xi} \, \mathrm{d}^3\boldsymbol{\eta} \, \mathrm{d}^3\boldsymbol{\zeta} \;. \qquad (31)$$

The simplest way to get the appropriate form of $U_m(r)$, fig. 6, is to include the first two terms of the expansion (27) with $a_3 > 0$ and $a_4 < 0$. Hence, the many-particle NN interaction includes at least the $3N$ repulsion and the $4N$ attraction. Of course, the presence of higher many-particle forces is not excluded. Therefore, the parameters a_3 and a_4 may be tentatively treated as effective quantities accounting for such forces. In this case they should be space-dependent, but the experimental accuracy is insufficient to reveal this dependence.

The above results are for the isoscalar part of the static field. The isovector part contains the $2N$ terms arising from the exchange by δ (scalar-isovector) and ρ (vector-isovector) mesons and the many-particle one $U_m^-(r)$. The above $2N$ terms are of close magnitude but different sign

thus greatly cancelling each other. For this reason the many-particle contribution appears to be the dominant part of the isovector potential. But in contrast to the isoscalar case the quantity $U_m^-(r)$ is found to be positive in the whole nuclear region. So its "many-particle structure" cannot be safely determined: the $3N$ forces are sufficient in this case

$$U_m^-(r) = a_3^- \rho(r)\rho^-(r), \qquad \rho(r) = \rho_n(r) + \rho_p(r),$$
$$\rho^-(r) = \rho_n(r) - \rho_p(r); \tag{32}$$

ρ_n and ρ_p are the neutron and proton density distributions.

The total static nuclear field is

$$U_{st}(x) = U_2(x) + a_3\rho^2(r) + a_4\rho^3(r)$$
$$-\tau_3\Big(U_2^-(x) + a_3^- \rho(r)\,\rho^-(r)\Big); \tag{33}$$

$\tau_3 = -1$ for neutrons and $+1$ for protons. The $2N$ terms consisting of scalar and vector fields (see ref. [3]),

$$U_2(x) = \gamma_0 S_2(r) + V_2(r) , \quad U_2^-(x) = \gamma_0 S_2^-(r) + V_2^-(r), \tag{34}$$

are calculated using the Bonn B [10] and the OSBEP [11] potentials, whereas the parameters a_3, a_4 and a_3^- are determined by the best-fit procedure [3] (the results for the spectra of doorway states are labelled as "full" in fig. 5). They are found to be

$$a_3 = 16.9296 \text{ fm}^5, \quad a_4 = -107.6744 \text{ fm}^8,$$
$$a_3^- = 3.6824 \text{ fm}^5, \tag{35}$$

when the Bonn B potential is used for the $2N$ forces and

$$a_3 = 17.0011 \text{ fm}^5, \quad a_4 = -110.3747 \text{ fm}^8,$$
$$a_3^- = 4.7346 \text{ fm}^5 . \tag{36}$$

for the OSBEP potential. More interesting are the values of the $2N, 3N$ and $4N$ contributions in the nuclear interior. Taking $\rho_0 = 0.17 \text{ fm}^{-3}$ for the average nucleon density in this region and $\rho_0^- = \frac{N-Z}{A} \rho_0$, we get

$$U_2 = -83 \text{ MeV}, \quad U_3 = +96.5 \text{ MeV}, \quad U_4 = -104 \text{ MeV},$$
$$U_2^- = 6\frac{N-Z}{A} \text{ MeV} , \quad U_m^- = 21\frac{N-Z}{A} \text{ MeV} \tag{37}$$

for the Bonn B potential and

$$U_2 = -82 \text{ MeV}, \quad U_3 = +97 \text{ MeV}, \quad U_4 = -107 \text{ MeV},$$
$$U_2^- = 0 , \qquad U_m^- = 27\frac{N-Z}{A} \text{ MeV} \tag{38}$$

for the OSBEP one. It is worth mentioning that the value of the potential in the nuclear interior is just the value of the force at the average distance r_0 between nucleons. Indeed, to get for instance the value of the $3N$ forces the volume integral a_3, eq. (30), must be divided by the square of the average volume per nucleon $V_0 = \frac{4\pi}{3} r_0^3$. But the quantity V_0^{-1} is just the average density ρ_0, so

$$f_3 = a_3 V_0^{-2} = a_3\rho_0^2 = U_3 \tag{39}$$

and the same for f_2 and f_4. In this way we see that the estimate (2) of the effective field theory does not apply to the genuine many-particle forces.
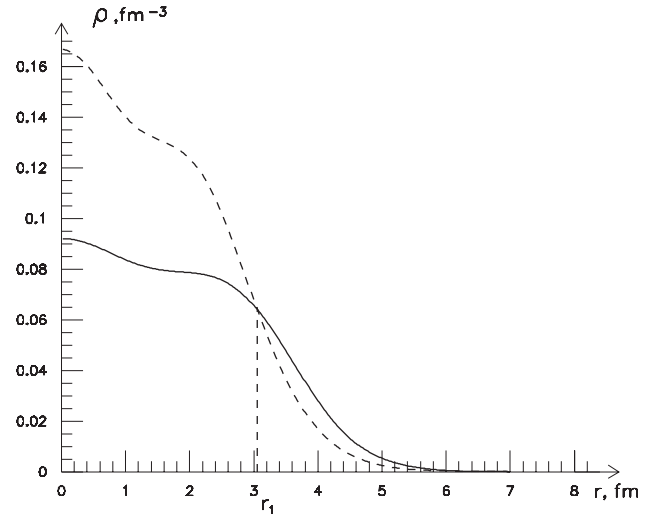
Fig. 7. Correlation-free (dotted line) and observed (solid line) proton density distributions in ^{40}Ca.

2.3 Correlations in nucleon density distributions

The correlation effects, owing to which the nuclear wave functions are different from Slater determinants, play an important role in nuclear phenomena. However, the exact methods of the treatment do not exist whereas the approximate ones are developed for the case of instantaneous two-particle forces only. For this reason the model-independent information about the magnitude of the correlation effects is not available at present. Such information, being important by itself, can be used as a test for more sophisticated methods taking into account both the many-particle nucleon-nucleon forces and the retardation effects (the latter ones may be of importance at higher densities).

The above information may be obtained in our approach by calculating the correlation-free quantities and comparing them with the observed ones [14].

Let us perform this for nucleon density distributions in nuclei. As a result of the correlations the occupation numbers n_λ of single-particle states are different from the Fermi step $\Theta(\varepsilon_F - \varepsilon_\lambda)$ and therefore a part of nucleons is out of the Fermi surface because the states with $\varepsilon_\lambda > \varepsilon_F$ are partly occupied. The number of such nucleons may be found by calculating the correlation-free density

$$\rho_{cf}(r) = \sum_\lambda \Theta(\varepsilon_F - \varepsilon_\lambda)|\varphi_\lambda(x)|^2 \tag{40}$$

and comparing it with the experimental one. This comparison is performed in fig. 7 for the proton density distribution in ^{40}Ca. As seen from the figure the correlation-free density contains more nucleons in the inner region $r < r_1$, the latter is the intersection point $\rho_{cf}(r_1) = \rho(r_1)$. The same result is obtained for neutron and proton densities

Table 1. N_{out} numbers in doubly closed-shell nuclei.

	^{16}O	^{40}Ca	^{90}Zr	^{208}Pb
Z_{out}	1.15	3.53	6.46	13.22
N_{out}	1.10	3.15	7.34	13.15
A_{out}	2.25	6.68	13.80	26.37
$A_{\mathrm{out}}/A, \%$	14	16.7	15.3	12.7

in all nuclei. The number of redistributed nucleons is

$$
\begin{aligned}
N_{\mathrm{out}} = {} & 4\pi \int_0^{r_1} \left[\rho_{\mathrm{cf}}(r) - \rho(r) \right] r^2 \mathrm{d}r = \\
& 4\pi \int_{r_1}^{\infty} \left[\rho(r) - \rho_{\mathrm{cf}}(r) \right] r^2 \mathrm{d}r .
\end{aligned}
\tag{41}
$$

This is just the number of nucleons out of the Fermi-surface because its depletion due to the correlations is the only reason for the redistribution. So the N_{out} numbers are the natural measure of the correlation effects in the density distributions.

The results of the calculations are shown in table 1. As seen from the table the number of such nucleons is rather large even for the doubly closed-shell nuclei. To our knowledge, this fact was first mentioned by Frankfurt and Strikman [15] on the basis of the analysis of inclusive deep inelastic lepton-nucleus scattering data at large values of the Björken scaling variable. According to their recent data [16] the ratio A_{out}/A is $(20 \pm 3)\%$ which is in reasonable agreement with our results.

3 Concluding remarks

Our main result is the demonstration of the possibility to observe the nonlinearity of strong interactions in nuclear experiments via the resulting many-particle nucleon-nucleon forces.

As seen from eqs. (36) and (37) the $3N$ and $4N$ forces are of the same magnitude as the $2N$ ones, but the signs of the many-particle forces are different. So the $3N$ and $4N$ forces greatly compensate each other. This is the possible reason for a relative weakness of the effective $3N$ forces as found in the calculations for few-nucleon systems, see sect. 1. But this near-compensation occurs at observed density values and it is hardly expected to be the case for higher densities. For this reason the contemporary results for the nuclear matter equation of state seem to be doubtful. More sophisticated methods taking into account the nonlinearity of strong interaction are necessary to get trustworthy results for the equation of state of nuclear matter.

The same concerns the calculations for few-nucleon systems because the contemporary methods do not apply in the presence of strong $3N$ and $4N$ forces. In particular, neither the Faddeev equations nor the Faddeev-Jakubovsky ones do apply in this case.

References

1. J.L. Friar, nucl-th/9911075; nucl-th/0005076.
2. A. Manohar, H. Georgi, Nucl. Phys. B **234**, 189 (1984); H. Georgi, Phys. Lett. B**298**, 187 (1993).
3. B.L. Birbrair, V.I. Ryazanov, Yad. Fiz. **63**, 1842 (2000).
4. H. de Vries *et al.*, At. Data and Nucl. Data Tables **36**, 495 (1987).
5. G.D. Alkhazov *et al.*, Nucl. Phys. A **381**, 430 (1982).
6. S.S. Volkov *et al.*, Yad. Fiz. **52**, 1339 (1990); A.A. Vorobyov *et al.*, Yad. Fiz. **58**, 1923 (1995).
7. A.A. Abrikosov, L.P. Gor'kov, I.E. Dzyaloshinsky, *Methods of Quantum Field Theory in Statistical Physics* (Prentice-Hall, Englewood Cliffs, 1963).
8. A.B. Migdal, *Theory of Finite Fermi-Systems and Applications to Atomic Nuclei* (Nauka, Moscow, 1983).
9. W.H. Dickhoff, E.P. Roth, M. Radici, nucl-th/0108028; W.H. Dickhoff, E.P. Roth, nucl-th/0108029; nucl-th/0108030.
10. R. Machleidt, K. Holinde, Ch. Elster, Phys. Rep. **149**, 1 (1987).
11. L. Jäde, H.V. von Geramb, Phys. Rev. C **57**, 496 (1998).
12. S.J. Wallace, Comm. Nucl. Part. Phys. **13**, 27 (1984).
13. J.D. Walecka, Ann. Phys. (NY) **83**, 491 (1974).
14. B.L. Birbrair, V.I. Ryazanov, Yad. Fiz. **64**, 471 (2001).
15. L.L. Frankfurt, M.I. Strikman, Phys. Rep. **76**, 215 (1981).
16. L.L. Frankfurt, M.I. Strikman, D.B. Day, M. Sargsyan, Phys. Rev. C **48**, 2451 (1993).